Research Journal of Applied Sciences, Engineering and Technology 6(23): 4470-4473, 2013
ISSN: 2040-7459; e-ISSN: 2040-7467

Submitted: March 01, 2013 Accepted: April 02, 2013 Published: December 15, 2013

Research on Aerodynamic Performance of an Wind Turbine Airfoil With Leading Edge Ice

[1]Fu Jie, [1]He Bin, [1]An Yi and [1, 2]Fan Qinshan
[1]Division of Mechanics, Nanjing University of Technology, Nanjing, China
[2]School of Aerospace, Tsinghua University, Beijing, China

Abstract: The performance of wind turbine was influenced by the environment. Among them, airfoil with leading edge ice has a great effect on the changes of aerodynamic performance. This study calculated the performance of an wind tubine airfoil at two iced shape model by CFD simulation using LES. LES in various models has been developed to simulate turbulent flows, especially to separated flows. In this investigation, 2D LES has been used to simulate flow past a wind turbine airfoil with leading edge ice which is a classical separated flow. The results show that flow structure is more complex with abundant whirlpools signifying violent turbulence when airfoil with ice and leads to poorer performance of wind turbine.

Keywords: Aerodynamic performance, full stall, leading edge ice, LES, separated flows, wind turbine ailfoil

INTRODUCTION

For the last decade the predominant configuration of modern wind turbines has been the three-bladed upwind pitch-controlled one. The researchers are often focous on the tubine power output. In all influence factors, the aerodynamic performance of blade is the dominant and complex one (Hansen, 2008). The response of the aerodynamic load depends on whether the boundary layer is attached or partly separated (Spera, 2009). Ice accretion can be a problem during certain weather which should be avoided due to the possible risk of decreased lift and increased drag on the blade. Some research shows that ice adhering to airfoil can cause severe problems, increased loads on the structural parts as well as altered aerodynamic behavior and changed the flow field structure increases the flow separations (Dalili *et al*., 2009). This is of course a subject of concern in regions with cold climate where the weather conditions make certain structures prone to ice accretion.

Accurate prediction of flow separation from airfoils is still a challenge for computational fluid dynamics today. As flow separation on airfoils is an undesirable phenomenon due to the fact that it is associated with lift breakdown and limits the usable range of the angle of attack. The reliable prediction of such flow configurations is great technical interest (Chao, 2006). As to the numerical studies, direct numerical simulations have good results for turbulent flows. But it needs more computational resources than LES for flow separation, transition, tip vortex and flow control (Tetsuro *et al*., 2007). Furthermore, LES has greater predictive potential than Reynolds-Averaged Navier-Stokes (RANS) methods.

In what follows, we study three airfoil models using 2DLES. One of the three model is standard airfoil. Another two models are airfoils with leading edge ice which summary frome from the literature (Hochart *et al*., 2008). The aim of this study is to provide an accurate simulation of the flow past a wind turbine airfoil in deep fall using a large eddy simulation in two dimensions and get detailed database to calculate the wind tuebine loads.

NUMERICAL APPROACH

2D-LES governing equations: The governing equations for LES of a neutrally stratified incompressible atmospheric boundary layer are the filtered Navier-Stokes equations:

$$\frac{\partial \bar{u}_i}{\partial \bar{x}_i} = 0 \tag{1}$$

$$\frac{\partial \bar{u}_i}{\partial t} + \frac{\partial \left(\bar{u}_i \bar{u}_j\right)}{\partial x_j} = -\frac{\partial \bar{P}}{\partial x_i} - \varepsilon_{ijk} f_j \left(\bar{u}_k - u_k^g\right) - \frac{\partial \tau_{ij}}{\partial x_j} \tag{2}$$

where turbulent stresses are defined as $\tau_{ij} = \overline{u_i u_j}$, f_j is the Coriolis parameter, e_{ijk} is the permutation tensor,

Corresponding Author: Fu Jie, Division of Mechanics, Nanjing University of Technology, Nanjing 21009, China

u_k^g is the geostrophic wind, $\bar{u}$ and $\bar{P}$ are the filtered velocity and filtered non-hydrostatic component of pressure, respectively (Kim *et al*., 2006).

In all simulations, we use periodic lateral boundary conditions and impose a stress-free condition on the upper boundary. At the lower boundary, the vertical component of velocity is set to zero and horizontal components of the turbulent stresses are defined based on the mean logarithmic wind profile assumption as follows 2DLES.

In two-dimensional incompressible turbulent flow, *f* is divided into two categories:

$$f = \overline{f} + f' \tag{3}$$

where $\bar{f}$ is large scale components, f' is small scale components:

$$f' = \iint_D \prod_{i=1}^{2} G_i(x_i, x_i') f(x_i, x_i') dx_1', x_2' \tag{4}$$

G_i (x_i, x_i') is Gaussian filter function in x_i:

$$G_i(x_i, x_i') = \left(\frac{6}{\pi\Delta_i^2}\right)^{1/2} \exp\left\{-6\frac{(x_i - x_i')^2}{\Delta_i^2}\right\} \tag{5}$$

where, $\Delta_{i=}\ h_i$, h_i is grid length in x_i, the continuity equation and Navier-Stokes equations are filtered with Eq. (5), the continuity equation and Navier-Stokes equations are filtered:

$$\frac{\partial \bar{u}_i}{\partial \bar{x}_i} = 0 \tag{6}$$

$$\frac{\partial \bar{u}_i}{\partial t} + \frac{\partial\left(\bar{u}_i \bar{u}_j\right)}{\partial x_j} = -\frac{\partial \bar{P}}{\partial x_i} + \frac{\partial}{\partial x_j}\left[\left(v + v_{SGS}\right)\bar{e}_{ij}\right] \tag{7}$$

where, $v_{SGS} = (C\Delta)^2 \left|\bar{e}_{ij}\right|$, (i, j = 1, 2): $\bar{e}_{ij} = \partial\bar{u}_i/\partial x_j + \partial\bar{u}_j/\partial x_x$; $\Delta = (\Delta_1\Delta_2)^{1/2}$; *C* is constants.

Numerical model and boundary condition:

Numerical model: The standard airfoil in this study is DU21 which is a member of the airfoil family DU, where 21 mean that the thickness of the airfoil is 21% chord. It has good aerodynamic performance and lift-to-drag ratio, mainly be used in the tail of wind turbine blade. Its airfoil-data coefficients were illustrated graphically in NREL technical report (Timmer and Van Rooij, 2003).

Figure 1 and 2 are the Grids of accreting rime and accreting glaze. Accreting rime and accreting glaze are

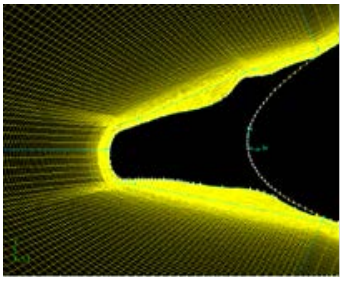

Fig. 1: Grid of accreting rime, case A

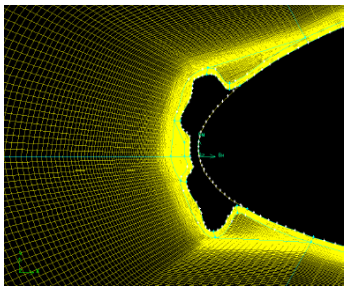

Fig. 2: Grid of accreting glaze, case B

the main forms of leading edge ice accretion. As can be seen from the picture, there are big differences between them at shape. For the purpose of improving the precision, the grid pattern was improved and locally refined.

Boundary condition: To capture the physics of vortex formation around the airfoil trailing edge and easy to comparative analysis the aerodynamic performance, Re = 2×10^6 (U_0 = 3 0 m/s, *C* (Chord Length) = 100 cm) and attack angles from 0° to 90° were numerically simulated by the 2D-LES. In the simulation, the flow field is calculated by using an C-H type grid system. The inlet boundary is placed five times chord length (5*C*) upstream of the leading edge of the blade while the outlet boundary is placed ten times chord length (10*C*) downstream of the trailing edge of the blade (Yoshihide and Ted, 2009).

RESULTS AND DISCUSSION

The aerodynamic characteristics of airfoil are mainly caused by the change of flow field. Figure 3 are Comparison of the flow field structure for three cases. (a) Is the streamlines of clean airfoil at attack of angle 15°, (b) is streamlines of case A, (c) is case B.

The streamlines show the development of the vortices at leading end trailing edge. Focusing on the trailing edge separation this happens sooner and more pronounced for ice B when comparing the individual angle of attack plots with the ones for the clean airfoil and ice case A. That means at some attack of angle, lift

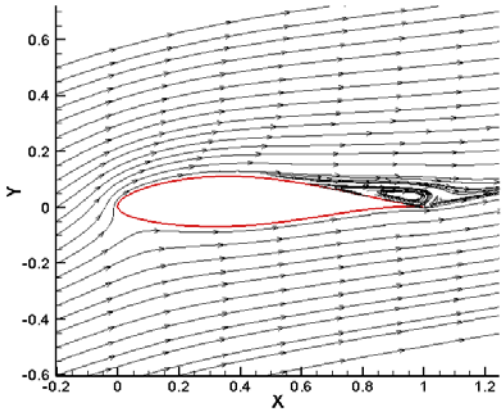

(a)

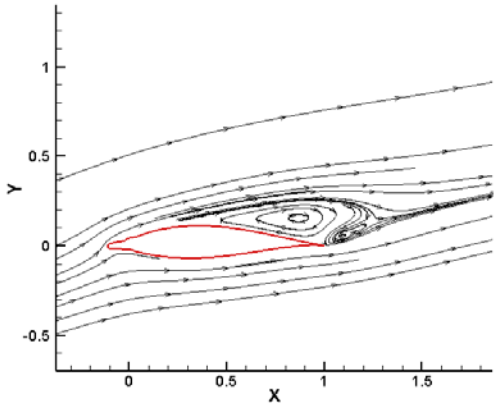

(b)

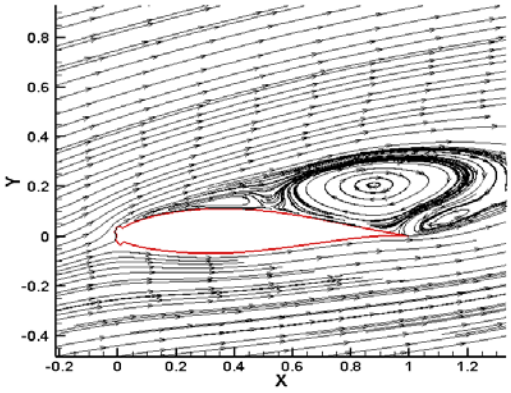

(c)

Fig. 3: Comparison of the flow field structure for three case at 15°

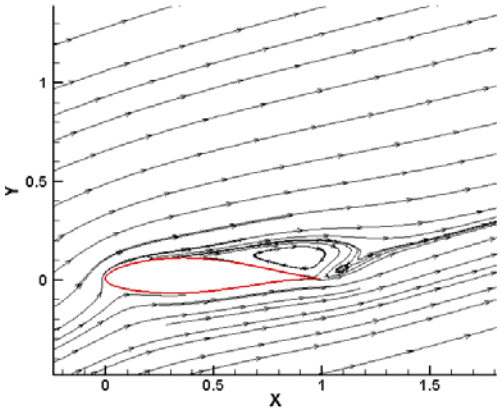

(a)

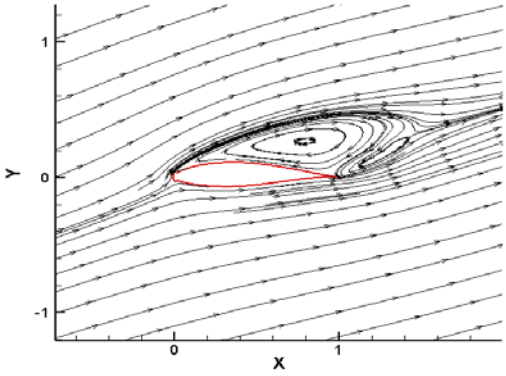

(b)

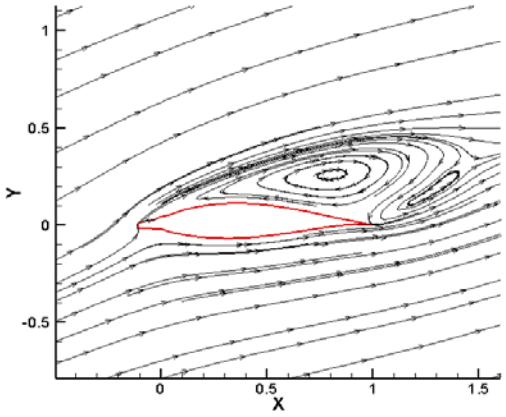

(c)

Fig. 4: Comparison of the flow field structure for three case 45°

coefficient of case B is more low and case A and case B have in deep stall.

As seen from Fig. 4a, at 45° angle of attack, clean airfoil trailing-edge vortex separation occurs, resulting in movement of the flow field near the airfoil stall. Full separation come up with the increase of initial attack angle at the same velocity for Case A and case B. We estimate the lift coefficient become much closer between case A and B (Fig. 4).

Figure 5 is comparison of the lift coefficient for three case at attack angle from 0 to 90. C_L of clean ailfoil generally agrees well with the compared results

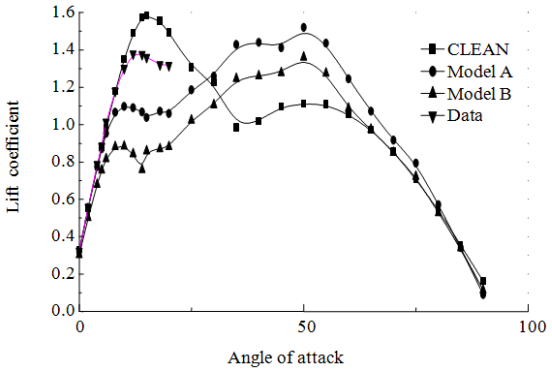

Fig. 5: Comparison of the lift coefficient for three case

from 0° to13°, CL increases with angle of attack until 15° where after there is flow in stall domain.

The horn-like protrusion shape severely affects the flow and thus the aerodynamic properties of the airfoil. It is obvious that the case A lift coefficient for all tubine work angles of attack (0°-30°) is lower than the clean airfoil due to the early leading edge separation and the more severe trailing edge vortices which developed at lower angles of attack than for the clean airfoil. The maximum CL of 1.05 is reached already at 11°.

It is seen that the lift coefficient is generally lower than both the clean airfoil and ice case A. C_L increases with angle of attack until 8° where after there is a decrease followed by another increase. The course of the curve with the lower angle of attack for maximum lift and the value for maximum lift corresponds well with the flow development described and compared to the clean airfoil and ice A above.

CONCLUSION

Two-Dimensional (2D) Large-Eddy Simulation (LES) and a hybrid RANS/LES were used to predict the flow past a wind turbine airfoil (DU21) at Re = 2×10^6 and angle of attack from 0° to 90° aiming at comparative analysis of their features and performance. In order to check their feasibility and get the aerodynamic performance of an airfoil with leading edge ice.

The lift coefficient of case A and B is generally lower than for the clean airfoil at most work angles of attack. Drag is increased compared to the clean airfoil due to the more severe separation resulting in increased pressure drag.

Ice case A and B changed the flow field structure and ailfoil aerodynamic performance. For wind turbine, the phenomenon cut down the power and added loads of blade and wind turbine foundation. In some places, we can't altered the climate, but in order to ensure the safe operation of wind turbine, we must consider this factor in the wind turbine blade design.

ACKNOWLEDGMENT

This study was financially supported by innovation project for graduates of Jiangsu Municipal Education Commission (CX10B_168Z).

REFERENCES

Chao, Q.L., 2006. High performance computation for DNS/LES. Appl. Math. Model., 30(10): 1143-1165.

Dalili, N., A. Edrisy and R. Carriveau, 2009. A review of surface engineering issues critical to wind turbine performance. Renew. Sust. Energ. Rev., 13: 428-438.

Hansen, M.O.L., 2008. Aerodynamics of Wind Turbines. James and James, London, pp: 95-96.

Hochart, C., G. Fortin, J. Perron and I. Adrian, 2008. Wind turbine performance under icing conditions. Wind Energy, 11(4): 319-333.

Kim, H.J., S. Lee and N. Fujisawa, 2006. Computation of unsteady flow and aerodynamic noise of NACA0018 airfoil using large-eddy simulation. Int. J. Heat Fluid Flow, 27(2): 229-242.

Spera, D.A., 2009. Wind Turbine Technology: Fundamental Concepts of Wind Turbine Engineering. 2nd., ASME Press, New York.

Tetsuro, T., C. Shuyang and O. Azuma, 2007. LES study of turbulent boundary layer over a smooth and a rough 2D hill model. Flow Turbul. Combust., 79(3): 405-432.

Timmer, W.A. and R.P.J.O.M. Van Rooij, 2003. Summary of the delft university wind turbine dedicated airfoils. J. Sol. Energ-T ASME, 125(4): 488-496.

Yoshihide, T. and S. Ted, 2009. Numerical simulation of dispersion around an isolated cubic building: Comparison of various types of k-ε models. Atmos. Environ., 43(20): 3200-3210.